108　Radar simulation studies for dual-frequency radar measurements of snow from space: Hydrometeor classification

Takahisa Kobayashi[1,3] , Mistuharu Nomura[1] ,Soichiro Sugimoto[1],Fumie Akimoto Furuzawa[2],

Ahoro Adachi[3] and Hiromaru Hirakuchi[1].

[1] Central Research Institute of Electric Power Industry,1646,Abiko,Chiba,Japan,270-1194

[2] Institute for Space-Earth Environmental　Research, Nagoya University , Chikusa-ku, Nagoya,Japan,464-8601

[3] Meteorological Research Institute, Tsukuba, Japan, 305-0035

1.　INTRODUCTION

The Dual Frequency radar (DPR) onboard the Global Precipitation Mission (GPM) core satellite operates at frequencies of Ku-band (14GHz) and Ka-band (35GHz). The DPR has the potential to measure more accurate rainfall rate than the space-borne precipitation radar (PR) operating at a single frequency on the TRMM satellite. The DPR is also useful for measuring snowfall rate, however, this is much more difficult than rain because radar received signals are affected by more microphysical parameters, such as size distribution, shape, volume fraction of water in snow as well as snowfall rate. Uncertainties of snowfall rate estimated from a single frequency radar has been reported to be as much as 75%.

As first step of measurements of precipitation, precipitation scatter should be identified as snow or rain. Currently, it is made by using estimated temperature which is not always correct. We, therefore developed a method for hydrometeor identification from the DPR signals. One of methods is to use a difference of received signals from the DPR. A radar operated at Ku-band detects signals in the Rayleigh regime, on the other hand, a radar at Ka-band detects signals in the Mie regime. In addition, Ka-band radar suffers more attenuation for rain than that for Ku-band radar. These different characteristics can be used to identify regions of dry snow and rain .

We have made simulations of radar received signals from rain and dry snow for the GPM-DPR configurations and have examined the dual frequency ratio (DFR: dBZe. (Ku)-dBZe (Ka)) which is frequently used to measure snow

* *Corresponding Author address*: Takahisa. Kobayashi,

Central Research Institute of Power Industry, 1646,

Abiko,　Chiba, 270-1194, Japan

e-mail : kobay@mri-jma.go.jp

(eg. Matrosov, 1998, Liao and Meneghini, 2011) . Here dry snow is defined as snow composed of ice and air. The purpose of our study is to examine the characteristics of the DFR and to develop a method to identify regions of dry snow and rain from the DFR for accurate measurements of precipitation.

2.　SIMULATIONS

The effective radar reflectivity Z_e is defined as

$$Z_e = \frac{\lambda^4}{\pi^5 |K_w|^2} \int_0^\infty \sigma_b N(D) dD. \qquad (1)$$

Here, λ is the wavelength of radar, σ_b the backscattering cross section, Kw is $(m^2-1)/(m^2+2)$ and m is the complex refractive index of water. D is the diameter of particles and $N(D)$ is the size distribution of particles (PSD). The DFR is defined here as,

$$DFR = Z_e(Ku:dBZ) - Z_e(Ka:dBZ). \qquad (2)$$

We have calculated the DFR for rain and snow of various microphysical properties.

2.1 Rain model

Shape of raindrops is assumed to be oblate and the axis ratio changes with the size for rain (Beard and Chung 1987). The size distribution of raindrops, N(D), can be expressed by an inverse exponential function, that is, Marshall-Palmer (M-P)　distribution as

$$N(D) = N_0 \exp(-\Lambda D). \qquad (3)$$

Here, N_0 is the intercept parameter. D is the volume equivalent diameter of raindrops. Shape parameter Λ (mm^{-1}) is related to rain rate (R:mm/h) as

$$\Lambda = 4.1 R^{-0.21} \quad . \qquad (4)$$

Temperature of rain and snow is assumed to be 273K.

2.2 Snow model

Snow model used in the present study is the so called soft oblate model: shape of snow was assumed to be oblate and the refractive index of snow was calculated assuming Maxwell-Garnet (M-G) theorem for various fraction of water in snow and size of snow. The axis ratio is assumed to be constant as 0.66. The size distribution can be expressed by a modified Gamma function as,

$$N(D_m) = N_0 D_m^{\mu} \exp(-\Lambda D_m), \qquad (5)$$

where, D_m is major axis of snow particles. Slope parameter μ is assumed to be 3. Shape parameter Λ (mm^{-1}) is related to the mean volume equivalent diameter (D_0). We assume snow as uniform mixture of ice, air and water and calculate the refractive index of a snow particle (m_s) by using the M-G theory. For dry snow, the refractive index (m_{ds}) can be expressed as

$$\frac{m_{ds}^2 - 1}{m_{ds}^2 + 2} = P_{ice} \frac{m_i^2 - 1}{m_i^2 + 2}, \qquad (6)$$

where, m_i is the refractive index of ice and P_{ice} is the volume fraction of ice in snow. For melting snow, the refractive index (m_{ws}) can be expressed as

$$m_{ws}^2 = m_{ds}^2 + 3P_w m_{ds}^2 \frac{m_w^2 - m_{ds}^2}{m_w^2 + 2m_{ds}^2 - P_w(m_w^2 - m_{ds}^2)}, \quad (7)$$

where, m_w is the refractive index of water and P_w is the volume fraction of water in snow.

For melting snow, the density ρ_{ws} is

$$\rho_{ws} = \frac{\rho_i \rho_w}{P_w \rho_i + (1 - P_w)\rho_w}, \qquad (8)$$

where ρ_i and ρ_w is the density of ice and water, respectively. Statistical studies of snow density suggest that mass of snow , M can be related to the size of snow (D)as,

$$M = aD^b. \qquad (9)$$

The coefficients a and b have been examined by many studies (Muramoto et al., 1995, Heymsfield et al. , 2004).

2.3 Calculation of the radar reflectivity

Scattering properties of rain and snow were calculated by using a radar simulator (GRASIA) by Kobayashi et al. (2011) which was originally developed for a polarimeteric radar. This model is a physically-based simulator in which the scattering properties of precipitation are calculated by using the T-matrix method (Mischenko,1998).

3. CHARACTERISTICS OF THE DFR

For rain of small size of raindrops, the scattering properties both at Ka and Ku-band radar are in the Rayleigh regime, which results in small values of the DFR unless attenuation occurs. For rain of large size of raindrops, the scattering properties at Ka-band radar is in the Mie regime but are still in the Rayleigh regime at Ku-band radar, which results in larger value of the DFR. For snow, on the other hand, the scattering properties are in the Mie regime both for Ka and Ku-band radar. Larger size of particles generally leads to larger values of the DFR. The DFR result from the different scattering properties of particles between Ka and Ku-band is called here as 'scattering effect'.

In addition to the scattering effects, attenuation due to rain results in increases in the DFR. Attenuation due to rain is not significant for Ku-band but is significant for Ka-band. This different attenuation property enhances the DFR. For dry snow, attenuation can be usually neglected both for Ka-band and Ku-band radar. It should be mentioned that "dry snow" is defined here as pure ice snow which is composes of ice and air. The DFR result from the different attenuation is related to rain rate and drop size and called here as 'attenuation effect'.

3.1 DFR in dry snow

Because of almost no snow attenuation at both 35 and 14 GHz, the DFR is determined by only the scattering effects for dry snow region. The scattering effects for dry snow are affected by snow density, PSD, shape, etc. The density is determined from the relationship between mass and size of snow flakes. Snow fall rate also affects the DFR because snow flake size usually varies with snowfall rate.

Figure 1 shows the radar reflectivity factor as a function of snow fall rate for various mass-size relationships at Ka-band (upper) and Ku-band (lower). The coefficients *a* and *b* for M-D relationship (Eq(9)) are applied by Matrosov (2007) for Model1, Heymsfield et al. (2004) for Model2, Locattelli and Hobbs (1974) for Model 3 and Muramoto et al. (1995) for Mode l4. The increases in the reflectivity at Ka-band are similar to that at Ku-band for various M-D relationships. These characteristics suggest that the effect of snow density on the DFR is expected to be not so significant (eg. Matrosov, 1998).

Figure 2 shows the DFR as a function of volume equivalent diameter (D_0) for various M-D relationships. Significant increases in the DFR with D_0 appear as expected. The effect of snow density is not so significant as mentioned above. These results suggest that the DFR primarily depends on the size of snow and secondly on the microphysical properties of snow like snow density.

3.2 DFR in rain

For rain, the DFR is determined by both the scattering and the attenuation effects. Figure 3 shows an example of a vertical profile of the DFR. The DFR due to the scattering effect (DFRs) increases slightly as height falls. The attenuation effects lead to significant increases in the DFR, in particular for lower altitude associated with increases in rain rate.

As mentioned above, the attenuation effects enhance the DFR significantly. The attenuation effects depend on rain rate and size of raindrops in the radar path. Attenuation, needless to say, increases with total rain rate in the radar path. The DFR due to the attenuation effects (DFRa), therefore, monotonically increase with the path integral rain rate. Attenuation by a raindrop also increases with size of a single raindrop. In the case of attenuation from a distribution of raindrops, however, differential attenuation between Ka and Ku-band does not change monotonically for given rain rate. Generally, larger size of raindrops has been observed for larger rain rate, which results in an increase of the attenuation with D_0.
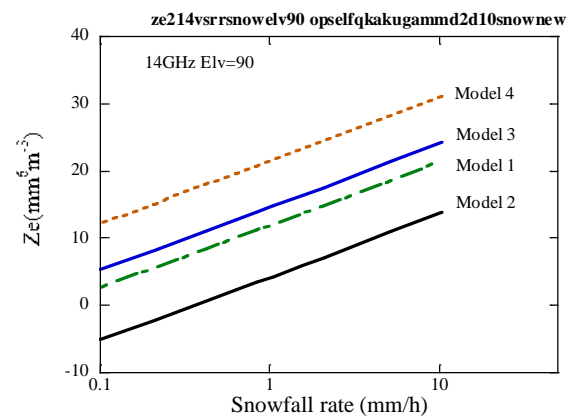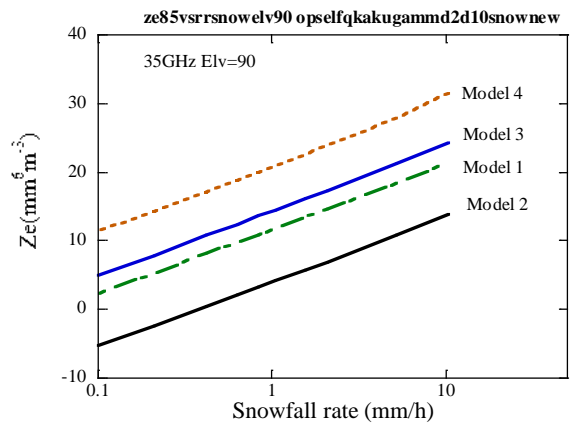
Fig. 1 The effective radar reflectivity factor at Ka(upper panel) and Ku(lower panel) for various M-D relationships.
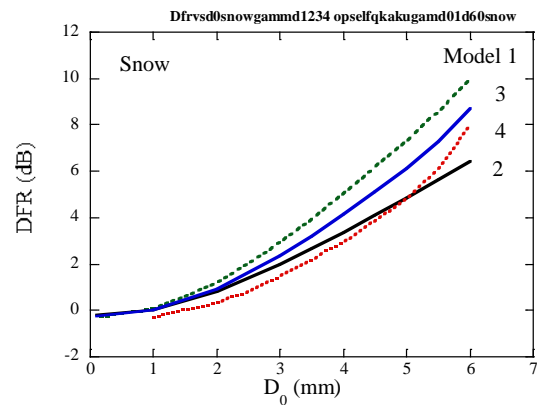
Fig. 2 The DFR versus D_0 for various M-D relationships.

Figure 4 shows the DFRs and the differential specific attenuation (Ka-Ku) as a function of D_0 for M-P size distribution. Small values of DFRs appear for small values of D_0 associated with the Rayleigh scattering regime both for Ka and Ku bands. The DFRs increases with size of raindrops. The differential attenuation also increases with D_0. This is because rain rate increases with D_0 for the M-P size distribution. The DFR, therefore, increases with D_0 by both the scattering and attenuation effects.

4. A CLASSIFICATION METHOD FOR RAIN AND DRY SNOW

The DFRs in rain region may be generally smaller than snow region because raindrops are usually smaller than snowflakes in size. For low snowfall rate, however, decreases in size of snowflakes are observed (Brandes et al., 2007), which results in decreases in the DFRs. In addition, the DFRa tends to increases downward direction due to the attenuation effects for rain. Similar values of the DFR are, therefore, often observed for rain and snow scatter.

Figure 5 shows the DFR versus Ze(Ku) for snow (upper panel) and rain (lower panel) measured with the GPM DPR around Japan. The DFR is independent of snow fall rate or Ze(Ku) a given for D_0. The measured DFR(DFRm), however, is clearly related to measured Ze(Ku) (Zem) which suggests that size of snowflakes tends to increase with snow fall rate. For rain, the DFRm similarly tends increases with Zem which results from more different specific attenuation with Zem and increases in size of raindrops with Zem. Similar values of the DFRm appear for snow and rain regions. It is, therefore, difficult to discriminate between snow and rain scatter from a single value of the DFRm.

A key factor for discrimination of snow and rain is the attenuation effects which tend to enhance the DFR and appear only in rain regime. We can, therefore, identify the scattering medium as rain if we can detect the attenuation

Fig. 5 The DFRm versus Zem(Ku) measured with GPM DPR for dry snow (upper panel) and rain (lower panel).
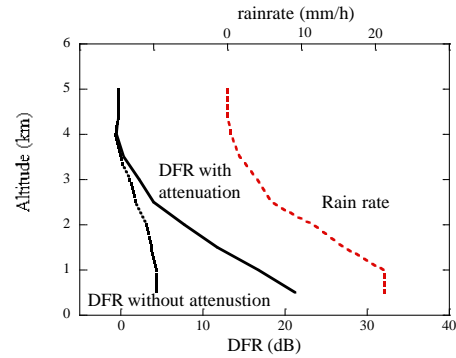
Fig. 3 Vertical profiles of the DFR and DFRs. Rain rate is also plotted.
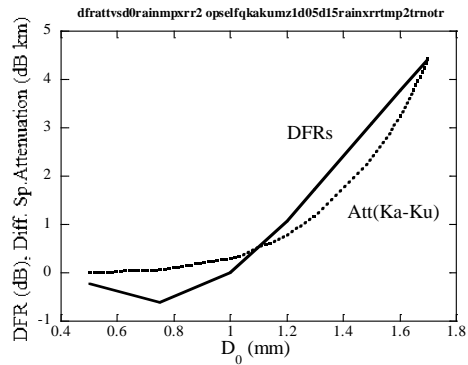
Fig. 4 The DFRs and differential specific attenuation versus D_0 .
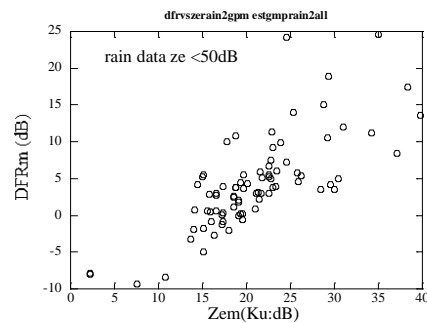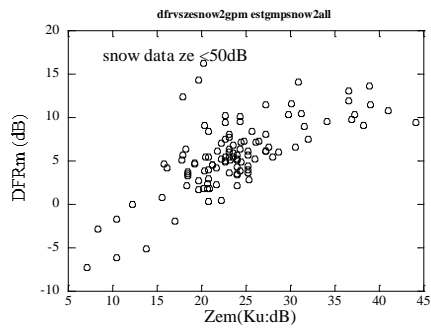
effects in the DFRm. To detect the attenuation effects, we should firstly remove the scattering effect in the DFRm. The scattering effects are basically related to the size of particles. Large values of the DFRs arise primarily from large particles in size. The increases in the size of particles are, generally, associated with higher precipitation rate, that is, larger value of Ze at Ku-band. The DFRs, therefore, can be expected to increases with Zem.

The attenuation effects are related to the rainfall rate and the size of raindrops. The increases in the size of raindrops are, generally, associated with higher rain rate, that is, larger value of Ze at Ku-band. These suggest that the ratio of the DFRm to Ze(Ku) is not constant but is a function of Ze and can be a measure of the attenuation effects. Variation of DFR/Ze with Ze(Ku) can be expected to be associated with the variation of DFRa/Ze in rain region. Variations of the ratio in snow region, are associated with changes in the size of snowflakes.

Figure 6 shows the ratio of the DFR to Ze(Ku) versus the difference between DFR and DFRs, that is, the DFRa. The ratio is linearly related to the difference except for DFR/Ze<0.1. Thus, the ratio of the DFR to Ze(Ku) is a measure of the DFRa. The scattering effects is expected to be removed by dividing DFRm by Zem to some degree.

Needless to say, the difference of the attenuation between Ka and Ku-band increases with radar path length. Thus the DFRa monotonically tends to increase toward downward direction, depending on the path integrated rain rate (PIR) from the top of rain layer to the observation altitude. Here, we will examine the changing tendency of the DFR/Ze(Ku) with the path integrated Zem (PIZ) from the top of rain layer instead of the PIR.

Figure 7 shows the DFR and the DFRs as a function of the PIZ for the vertical profile of rain shown in Fig.3. Increasing tendency clearly appears for the DFR, while no clear changing tendency appears for the DFRs. Thus, we can identify the scatter as rain region if continuous data of the ratio of DFRm/Zem increase with the PIZ in specified layer. It should be mentioned that we cannot identify snow or rain at a specified altitude but at a specified layer.
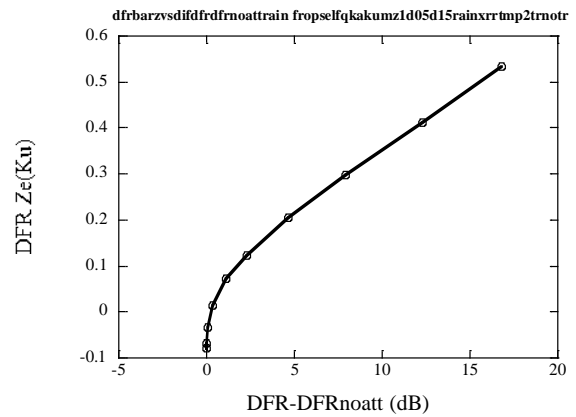
Fig. 6　The ratio of DFR to Ze at Ku-band versus difference of DFR and DFRs.
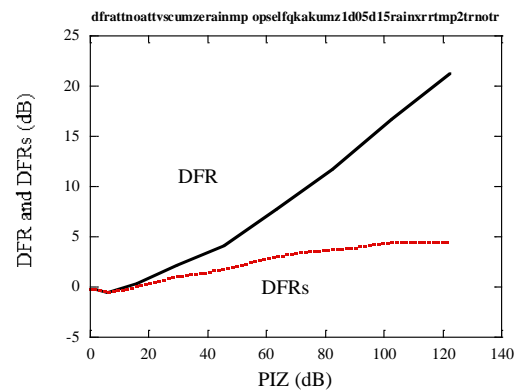
Fig. 7 The DFR and DFRs versus PIZ.
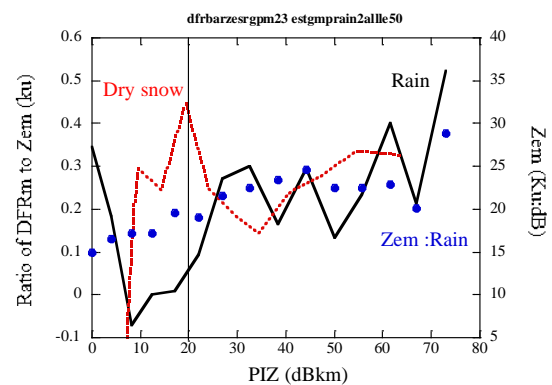
Fig.8 The ratio of DFRm to Zem at Ku-band versus PIZ for snow(red) and rain (black) region. Zem at Ku-band (blue dots) are also plotted.

We have applied the classification algorithm to data measured with the DPR. To identify rain region, we need to examine changing tendency of the consecutive data of the DFR. Figure 8 shows the DFRm/Zem(Ku) versus PIZ (dBkm) for snow(red line) and rain (black) in the altitude of 2 to 3km above msl. For Zem(Ku) (blue dots) larger than 20dB, the ratio tends to increase with PIZ for rain, while no clear tendency appears for snow.

5. CONCLUSIONS

We have proposed a method to identify regions of dry snow and rain from sequential data of the DFRm and Zem(Ku). Because the attenuation effects appear only in rain region, we can identify the scattering medium as rain if we detect the attenuation effects in the measured DFRm. The ratio of the DFRm to Zem(Ku) is thought to be a measure of the attenuation effects in rain region. The changes in the ratios in snow regions are associated with changes in the size of snowflakes. The ratio is, therefore, expected to increase with PIZ for rain region. We examined the algorithm for measured data with the GPM-DPR. Increasing tendency of the ratio appears for rain region.

References

Beard, K. V., and C. Chuang, 1987: A new model for the equilibrium shape of raindrops. J. Atmos. Sci.,44, 1509-1524.

Brandes. A., K. Ikeda, G. Zhang, M. Schonhuber,   and R. M. Rasmussen,   A Statistical and Physical Description of Hydrometeor Distributions in Colorado Snowstorms Using a Video Disdrometer, *J. Appl. Meteor. Clim.*, 46, 634-650, 2007.

Heymsfield, A.J., A. Bansemer, P. R. Field, C. Schmitt, C. Twohy, and M. R. Poellot, 2004, Effective ice particle densitys from aircraft data, *J. Atmos. Sci.*, 61,982-1003

Kobayashi,T., and K. Masuda, H. Yamauchi, and A. Adachi, 2011, Physically-based Simulator for   measurements of precipitation with Polarimetric and Space-borne Radars, SPIE Remote Sensing, Cheko, Praha 9/18-9/24, 2011.

Liao, L., and R. Meneghini, 2011, A study on the feasibility of dual-wavelength radar for identification of hydrometeor phases, *J. Appl. Meteor. Clim*, 50, 449-456

Locatelli, J. D., and P. V. Hobbs, 1974: Fall speeds and masses of solid precipitation particles. *J. Geophys. Res.,* **79,** 2185–2197.

Matrosov, S. Y., 1998, A dual-wavelength radar method to measure snowfall rate. *J. Appl. Meteor.*, 7, 1510-152

Matrosov, S. Y., 2007, Modeling backscatter properties of snowfall at millimeter wavelength, *J. Atmos. Sci.*, 64,1727-1736.

Mischchenko, M. I.,"Capabilities and limitations of a current fortran implementation of the T-matrix method for randomly oriented ,rotationally symmetric scatters", *J. Quant. Spectrosc. Radiat. Transfer*, 60, 309-324(1998).

Muramoto, K.-I., K. Matsuura, and T. Shiina, 1995: Measuring the density of snow particles and snowfall rate. *Electronics and Communications in Japan,* Part 3, Vol. 78, 71–79.